Study protocol with statistical analysis plan

Official Title: A Novel Method to Detect Pulmonary Thromboembolic Events with Non-Contrast 4DCT

NCT number: 03183063

Document Date: March 29, 2018

A Novel Method to Detect Pulmonary Thromboembolic Events with Non-Contrast 4DCT

IRB NUMBER: 2017-018
IRB APPROVAL DATE: 04/19/2018

1.0 Introduction

Acute Pulmonary Embolism

Deep vein thrombosis (DVT) occurs when a blood clot forms in a deep vein, typically in the lower extremities. Pulmonary embolism (PE) occurs when a DVT clot (or fragment) breaks free and travels through the heart to the pulmonary arteries and lodges in an artery causing complete or partial obstruction. Together DVT and PE comprise venous thromboembolism (VTE), a major public health problem in the United States (USA). VTE is the third leading cause of cardiovascular death (1), is estimated to result in 5% to 10% of all hospital death (2), and the third most common cause of preventable hospital death in patients recovering from surgery (3). Using the 2007-9 National Hospital Discharge Survey data, 548,000 hospitalizations were for VTE and of those 278,000 were for acute PE (4). The annual cost of VTE to the US healthcare system is $7-10 billion for newly diagnosed, medically treated VTE cases (5). PE is associated with a high short-term mortality, requiring a timely and accurate diagnosis for the initiation of antithrombotic therapy. PE is difficult to diagnose on presentation due to the non-specific signs and symptoms for this condition such as cough, shortness of breath, hypoxia, tachycardia, and hemoptysis.

Computed Tomography Angiography

Pulmonary computed tomography angiography (CTA) is the gold standard for the detection of pulmonary emboli (PE) (6), however, radiation exposure and complications related to administering intravenous contrast prohibit universal applicability (7). CTA can detect acute PE with a sensitivity of 90 percent and specificity of 95 percent when combined with CT venography (8, 9). In those who are medically ineligible for CTA, ventilation-perfusion (V/Q) single photon emission computed tomography (SPECT) imaging is commonly acquired to detect PE (10, 11). However, SPECT imaging acquisitions requires transporting the patient to the nuclear medicine clinic, a prolonged acquisition period compared with CTA, and in many hospitals SPECT imaging is not available on weekends or evenings. In this study we will investigate an alternative method to obtain ventilation and perfusion images from respiratory gated non-contrast CT (commonly called 4DCT) that can be performed in the Emergency Department.

^{99m}Tc-MAA SPECT Imaging

Wagner reported the first use of radiolabeled macroaggregates of albumin (MAA) imaged with planar scintigraphy for the detection of pulmonary emboli (PE) causing vascular occlusion (12). MAA is composed of particles ranging in size from 10 to 150 μm that are trapped in the pulmonary microvasculature on their first pass after intravenous injection. Their distribution remains fixed with a biological half-life of 11 h and is dependent on the conditions at the time of injection. ^{99m}Tc-labelled MAA (^{99m}Tc-MAA) imaged with single photon emission computed tomography (SPECT) is considered the standard method for the quantitative determination of pulmonary perfusion (13). Alternative pulmonary perfusion imaging methods include positron emission tomography imaging following administration of ^{68}Ga-labeled particles or after bolus injection of ^{13}N-N_2 (14). Magnetic resonance imaging (MRI) with contrast agents have been utilized experimentally to image the pulmonary vasculature and tissue perfusion (15). Quantification of SPECT images requires correction of the acquired data for attenuation and scatter (16, 17). One approach is to utilize spatially correlated CT images to determine the attenuation correction, which has lead to the development of SPECT-CT scanners (18). The low-dose CT can be utilized to evaluate the lung airway architecture, lung parenchyma, and pleural space in conjunction with the registered perfusion images rivaling CTA in sensitivity and specificity (19).

Variation in Pulmonary Perfusion with Breathing

In a recent study using ^{99m}Tc-MAA SPECT imaging, the difference in distribution due to injection at maximum inspiration versus maximum expiration breath-hold was measured (20). Each subject received SPECT imaging after injection of ^{99m}Tc-MAA in either maximum inspiration or expiration. There was a posterior displacement of the activity centroid in each lung between the expiration

and inspiration images. In another study of normal volunteers MRI perfusion imaging obtained at either maximum inspiration or expiration breath-holds revealed higher perfusion at expiration (15). In a study comparing CT attenuation with SPECT perfusion defects, patients were found to have hypo-attenuated pulmonary regions corresponding to regions with decreased perfusion in 57% of acute pulmonary emboli and 88% of chronic emboli cases (21). In the same study hyper-attenuated regions were found to correspond to regions with hyperperfusion. A method to measure pulmonary perfusion based on subtraction digital fluoroscopy without contrast has been reported (22). In that study subtraction images were generated between chest projection images at systole and diastole generating an image representing the perfusion difference. These perfusion projection images were correlated with ^{99m}Tc-MAA scintigraphy. Thus, changes in the amount and distribution of pulmonary perfusion throughout the respiratory cycle can be expected and these changes may be apparent on dynamic CT.

Imaging Pulmonary Perfusion Defects with 4DCT

Simon (23) described a technique to calculate the change in fractional content of air within pulmonary tissue between anatomically matched CT regions based on a simple model that assumes the density changes were solely due to air content (see appendix A in (24)). We successfully applied that model to inhale & exhale breath-hold CT image pairs (25) as well as 4DCT images (24, 26) to create ventilation images. However, the amount of blood in the thorax and lungs varies with the respiratory cycle increasing with inspiration during normal breathing (27) and decreasing with inspiration with positive pressure ventilation (28). Thus violating the assumption of the model. We found a cyclic variation in the apparent weight of the lung on 4DCT (see figure 1 below (26)) and others have reported respiratory induced variations in pulmonary perfusion of the lung on magnetic resonance imaging (MRI) (29). The pulmonary density changes found on 4DCT thus result from both changes in air and blood content.

4DCT derived ventilation images can also be inferred from the respiratory motion induced local tissue volume changes (24) independent of the 4DCT density values. The Jacobian determinant of the deformation field, calculated from the DIR result of images depicting different respiratory phases of the lungs, is used to estimate the local volume changes or ventilation (24, 30). There is a discrepancy between the density based and the Jacobian based ventilation images suggesting a method to extract respiratory induced blood mass change from 4DCT images. We hypothesize the respiratory induced blood mass change will only occur within perfused lung regions. Each 4DCT image set contains information representing the density change resulting from both ventilation and respiratory induced blood mass changes. Extracting both ventilation and a perfusion-like image from the 4DCT image intensities, referred to as Hounsfield Units (HU), is our goal. However, novel image processing methods are required to extract this information.

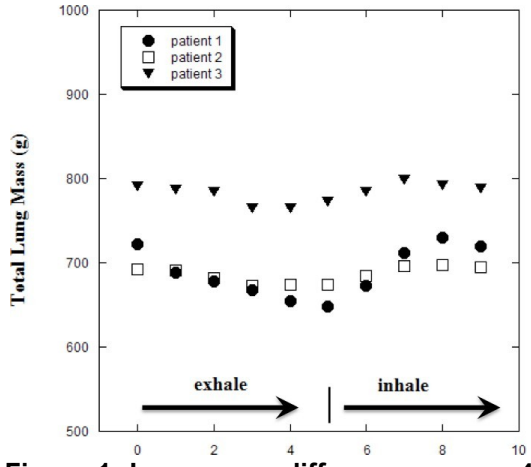

Figure 1. Lung mass difference across 4D CT. The total mass of the lung parenchyma (HU < –250) for each patient (p1-3) was calculated within the manual segmented lungs from the CT values and equation. Note there are difference between the three patients' data in amplitude and average value.

We found a cyclic variation in the apparent mass of the pulmonary parenchyma (Figure 1) (26). We hypothesize this variation is due to changes in pulmonary perfusion from the respiratory-induced variation in cardiac output (20, 31, 32). We

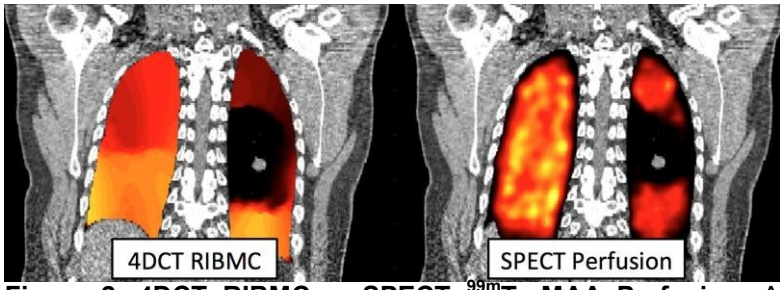

Figure 2. 4DCT RIBMC v. SPECT ^{99m}Tc-MAA Perfusion. A coronal section is shown from a 4DCT derived RIBMC images for a patient with malignant airway stenosis (Left). The corresponding ^{99m}Tc-MAA SPECT coronal section is shown (Right). The cold spot in the RIBMC image coincides with the perfusion defect in the SPECT perfusion image.

hypothesize this respiratory induced blood mass change will allow the identification of hypoperfused lung regions. As a preliminary study we created 4DCT RIBMC images from cases with hypoxia induced vasoconstriction, patients with malignant airway obstruction. The resulting images visually compare well with SPECT ^{99m}Tc-MacroAggregates of Albumin (MAA) perfusion images (Figure 2). However, in these cases there are matched ventilation and perfusion defects due to malignant airway obstruction. It is unknown if this process works to detect perfusion defects due to pulmonary emboli, where perfusion is obstructed and ventilation normal.

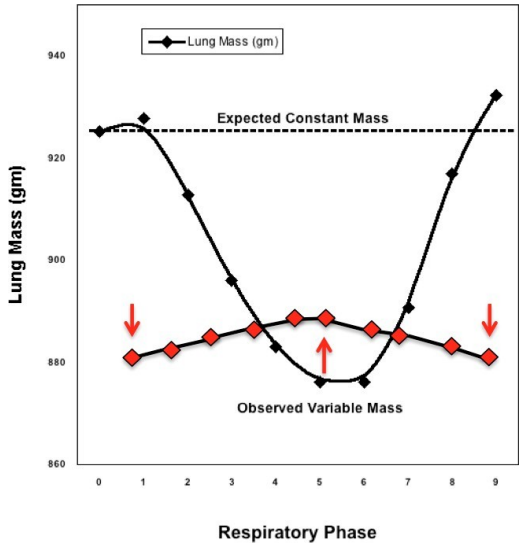

Figure 3. Effect of Positive Pressure Ventilation. . Hypothetical expected changes to previously mentioned trends in blood mass observed with spontaneous breathing if the patients are scanned during positive pressure ventilation, such as BPAP.

With spontaneous tidal breathing, venous return to the right atrium increases with the decrease in intrathoracic pressure (33) and as a consequence pulmonary arterial blood flow to the lungs increases (34). With positive pressure ventilation the opposite occurs, positive-pressure inspiration decreases the pressure gradient for venous return, which decreases venous blood flow, RV stroke volume, and consequently cardiac output (33). We expect the decrease in lung mass, or pulmonary blood, with normal expiration to become an increase in lung mass with positive pressure ventilation as shown in Figure 3 at the right.

In this study, patients found to have new segmental, lobar or greater perfusion defects, will be imaged with ^{99m}Tc-MAA SPECT/CT and 4DCT to compare perfusion with RIBMC defects.

Hypothesis: Thromboembolic pulmonary perfusion defects on ^{99m}Tc-MAA SPECT/CT will coincide with 4DCT RIBMC defect regions.

Summary & Significance

This is a prospective imaging trial of 20 patients with segmental or lobar pulmonary emboli on CTA. Each will receive ^{99m}Tc-MAA SPECT/CT and 4DCT imaging on the same day. Respiratory induced blood mass change (RIBMC) images will be derived from the 4DCT image and quantitatively compared with the SPECT perfusion images. A 5 patient cohort (cohort 2) to test effect of respiratory pressure on RIBMC was added. A 124 patient cohort (cohort 3) to test the sensitivity & specificity of RIBMC was added. Illustrated in Figure 4 below.

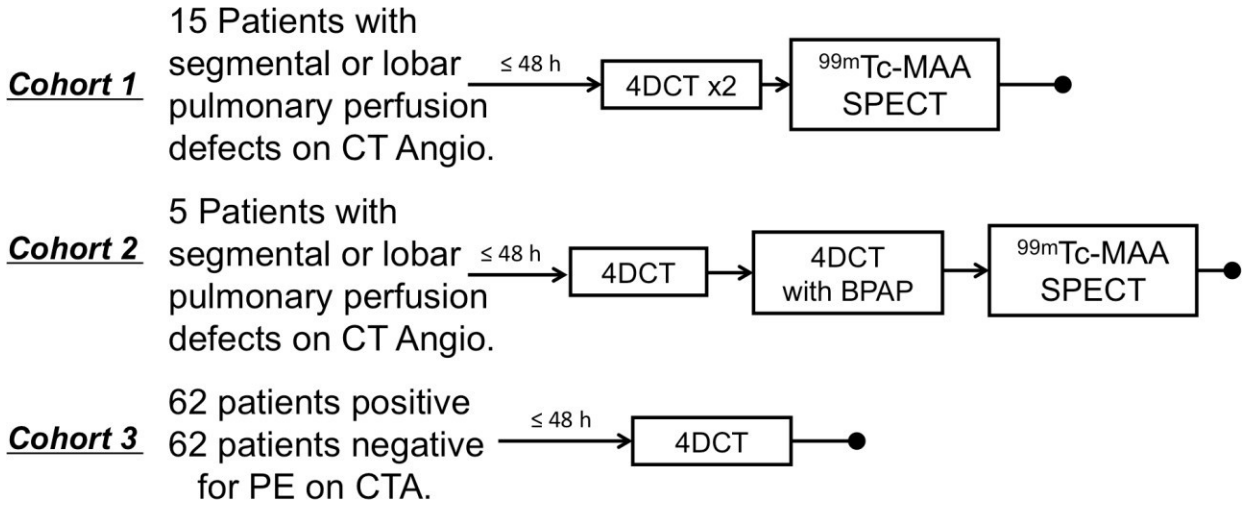

Figure 4. Study design. 15 patients (cohort 1) found to have segmental or lobar pulmonary emboli on CTA will be recruited for this study. All enrolled subjects will receive ^{99m}Tc-MAA SPECT/CT and 4DCT imaging. The 4DCT acquisitions will be performed at a single setting to evaluate reproducibility, prior to the SPECT/CT imaging. The primary end-point will be the identification and spatial correspondence of pulmonary perfusion defects on the ^{99m}Tc-MAA SPECT/CT and 4DCT derived RIBMC images. All imaging will be performed on the same day. An additional 5 patients (cohort 2) with the same criteria will be recruited. Each will receive ^{99m}Tc-MAA SPECT/CT imaging as before. They will also receive two 4DCT acquisitions, one with normal breathing and the other with positive pressure breathing using BPAP. 62 patients (cohort 3) found to have PE on CTA and 62 patients negative for PE will be recruited for this study. All enrolled subjects will receive a single 4DCT image acquisition. The 4DCT acquisitions will be performed within 48 hours of the CTA.

2.0 Objectives

2.1 The primary objective of this study is to test if 4DCT derived RIBMC images can detect segmental or lobar pulmonary perfusion detects.

2.2 A secondary objective is to evaluate the reproducibility and variability of RIBMC images on repeat imaging.

2.3 To evaluate the pulmonary blood volume response to positive pressure ventilation versus spontaneous breathing.

2.4 The primary objective of cohort 3 is to assess the sensitivity and specificity of contrast-free 4DCT functional imaging for detection of pulmonary emboli.

3.0 ELIGIBILITY, RECRUITMENT, AND SELECTION

Patients with CTA proven segmental of lobar pulmonary emboli will be recruited for this study. Subjects will not be excluded based on age, gender, gender identity, sexual orientation, economic status, race or ethnicity.

3.1 One cohort of 15 patients and another of 5 patients (20 patients total) with CTA proven segmental of lobar pulmonary emboli will be consented for the study and registered on the protocol. Patients may have started anti-coagulation therapy prior to enrolling.

3.1.1 Inclusion Criteria

3.1.1.1 Patients with segmental of lobar pulmonary emboli on CTA identified within past 48 hours.

3.1.1.2 May have initiated anticoagulation therapy.

3.1.1.3 Patients must sign informed consent to enter this study.

3.1.1.4 Documented not pregnant if child-bearing age woman.

3.1.2 Exclusion Criteria

3.1.2.1 Patients unable to tolerate two 15-minute (4DCT) and one 30- minute imaging sessions (SPECT/CT) in the same day.

3.1.2.2 Unable to sign informed consent due to cognitive impairment or health status.

3.1.2.3 Patients who are unstable from a respiratory status requiring ICU care.

3.1.2.4 Patients who receive tissue plasminogen activator.

3.1.3 Patients who are <18 years old.

3.2 One cohort of 124 patients who present to the Emergency Center with suspected pulmonary emboli. We will recruit patients 62 positive and 62 negative for pulmonary emboli on CTA.

3.2.1 Inclusion Criteria

3.2.1.1 Patients who are scheduled to receive, or who have received, CTA for suspected pulmonary emboli within past 48 hours.

3.2.1.2 May have initiated anticoagulation or tissue plasminogen therapy.

3.2.1.3 Patients must sign informed consent to enter this study.

3.2.1.4 Documented not pregnant if child-bearing age woman.

3.2.2 Exclusion Criteria

3.2.2.1 Patients unable to tolerate one 15-minute (4DCT).

3.2.2.2 Unable to sign informed consent due to cognitive impairment or health status.Patients who are <18 years old.

4.0 STUDY EVALUATIONS

Study patients will receive 4DCT imaging after signing consent, followed by ^{99m}Tc-MAA SPECT/CT, and a second 4DCT imaging session.

4.1 4DCT ACQUISITIONS*. The patients will be imaged lying supine and flat on the scanner bed with their arms above their head. On a multislice CT scanner, CT images will be obtained through the entire lung during resting tidal breathing while the patient's respiration is monitored with an external device for respiratory gating using the standard over-sampled spiral 4DCT acquisition method (35, 36). The 4DCT acquisition will be acquired in duplicate at standard low dose.

4.2 4DCT ACQUISITIONS W/ BPAP. The patients will be fitted with a face mask covering mouth and nose. The expiratory positive airway pressure (ePAP) will be set to 4 cm H_2O and inspiratory positive airway pressure (iPAP) to 12 cm H_2O. A 4DCT will acquired as described in the previous section. The patients will undergo BPAP for <10 minutes. Upon completion of the scan the patients will resume normal breathing of room air.

4.3 ^{99m}Tc-MAA SPECT/CT ACQUISITIONS*. The patients will undergo ^{99m}Tc-MAA SPECT/CT pulmonary perfusion imaging in the nuclear medicine clinic using the

standard clinical procedure under the supervision of a Beaumont nuclear medicine physician. This will include SPECT/CT imaging using ^{99m}Tc-labeled macro-aggregated albumin (^{99m}Tc-MAA), an FDA approved radiopharmaceutical in routine clinical use at Beaumont. The dose and administration will be prescribed by the nuclear medicine physician. A CT will be acquired for attenuation correction and image registration purposes and is a standard part of this procedure. The patients will be imaged supine with arms above their head. This scan will be performed on the same day as the 4D CT scans.

*If any incidental findings are noted, that have not been previously reported, the researcher will discuss these with the patient's treating clinical physician who will determine appropriate follow up.

5.0 CRITERIA FOR STUDY REMOVAL

5.1 Unacceptable adverse event (at the discretion of the treating physician).

5.2 Patients unable to tolerate imaging sessions (1 hour total).

5.3 Patient choice (patients can withdraw from the study at any time, for any reason).

5.4 Patients who's image quality does not meet criteria for primary endpoint analysis due to imaging techniques, scanner settings, patient movement, etc…

6.0 REGISTRATION PROCEDURES

6.1 Informed consent is required prior to participation in this study. The study coordinator will inform potential subjects about the study opportunity and ask if they would like to participate. If the patient is interested, they will be given an opportunity to read the informed consent and authorization document specific to the study and ask questions of the study coordinator. The patient will be informed about: 1) the rationale for the study; 2) the logistics of the study; 3) the risks of the study; 4) how the data will be used. Consent will be obtained by the study coordinator. The patient will be given a copy of the consent, and asked to sign another copy for our records.

6.2 Patients will be registered for the study after pretreatment evaluation is completed and eligibility criteria are met.

6.3 The principal investigator and all key personnel have completed NIH approved institutional and HIPAA training in the conduct of medical research studies

7.0 STATISTICAL CONSIDERATIONS

Spatial overlap between hypoperfused regions of interest (ROIs) on SPECT perfusion (standard) and deficit ROIs on RIBMC will be assessed using Dice similarity coefficient (DSC) (37). *A priori*, we expect a DSC of approximately 0.7 between RIBMC and SPECT ROIs. Indication of larger overlap is desirable for RIBMC validation. Thus, we require a DSC of at least 0.85 (38) and base our sample size calculations on this degree of improvement over *a priori* expectations. With three experts delineating ROIs on RIBMC and SPECT images, we will calculate an average (n = 3 experts) DSC per patient. Sample size considerations are based on a t-test for the mean DSC. Castillo et al. (39) provide a working DSC standard deviation of ~0.2, leading to a standard deviation of 0.11 ($=0.2/\sqrt{3}$) for a mean DSC based on three experts. Assuming a significance level of .05, power of 95%, and standard deviation of 0.11, we find that 15 patients are required to detect a mean DSC of at least 0.85.

Cohort 3. The objective of this study is to collect and process the image data necessary to assess the sensitivity and specificity of our CT Functional Imaging (CT-FI) diagnostic test, consisting of RIBMC and 4DCT-Ventilation, as well as perform receiver operator

characteristic (ROC) analysis. We will conduct a prospective imaging study of 124 patients who present to the Emergency Department with clinical concern for PE and who subsequently undergo chest CTA for further evaluation.

For each case, an expert reader will determine if functional deficits exist within CT-V and RIMBC. The patient will be classified as PE positive if the reader confirms the presence of two or more mismatched segmental or subsegmental defects between CT-V and RIBMC images, and negative otherwise. This CT-FI binary classification indicator will be acquired for each patient. Sensitivity and specificity will be computed with respect to the known (CTA defined) PE diagnosis. A score of 1 (low) to 5 (high) will be assigned to each defect for the ROC evaluation.

Because PE status of the subjects will be known a priori, we may use the statistical theory for estimating a single proportion to determine the sample size needed to estimate the sensitivity or specificity of the CT-FI diagnostic test. Assuming that the sensitivity will be (at least) approximately 80%, we can estimate the true sensitivity with a margin of error of 10% (percentage points) with 95% confidence based on a sample size of 62 positive PE cases. Similarly, the specificity can be estimated with 62 negative PE controls. Concerning the ROC analysis, to determine the sample size needed to detect an "Area under the ROC Curve" (AUC) greater than 50%, it is not necessary to have a prevalence value for PE (since PE status is known a priori). To detect an AUC of at least 70% with Type I error of 1%, power 95% and a 1:1 ratio of cases:controls we require at least 60 cases and 60 controls (40). Our study is designed to exceed the minimal sample size requirements.

8.0 POTENTIAL RISKS

The patients recruited for enrollment in this study will consist of patients who were found to have pulmonary emboli on diagnostic CTA. Their participation in this study will consist of ^{99m}Tc-MAA SPECT/CT imaging once and 4DCT imaging twice. The total dose per patient for this study is estimated at 44.2 mSv. This dose is less than the Radiation Safety Committee guidelines of 50 mSv per year from research.

8.1 SPECT/CT tests. The patients recruited to this study will have ^{99m}Tc-MAA SPECT/CT imaging at study entry. No changes are made to the clinical SPECT/CT imaging techniques specified by this study. A SPECT/CT imaging may cause a feeling of claustrophobia while lying in the scanner. The scanner is open at both ends and an open dialogue with doctors and staff will be maintained to minimize this risk. SPECT/CT imaging utilizes ionizing radiation. The radiation dose will be approximately 4.2 mSv. The radioactive isotope ^{99m}Tc-MAA has a half-life of 6.0 hours due to physical decay along with a biological clearance.

8.2 4DCT test. The major risk from the two 4DCT scans is from the radiation. Each 4DCT scan will deliver approximately 10-20 mSv to the patient. Erring on the high side of this range, this will befor a total of 40 mSv.

9.0 LONG TERM GOALS

This study investigates the use of 4DCT, an imaging study that can be rapidly performed in the emergency department without the need for contrast, in the evaluation of PE.

9.1 If successful, this strategy may be tested in further prospective studies in patients who have an unknown PE status.

9.2 4DCT RIBMC images may provides a means to detect pulmonary perfusion defects rapidly, at low radiation dose, and in patients who cannot receive intravenous contrast.

9.3 Determine the sensitivity and specificity of 4DCT RIBMC images to detect pulmonary emboli.

10.0 DATA MONITORING & ADVERSE EVENT REPORTING

10.1 Data Monitoring. The Data and Safety Monitoring Plan (DSMP) is established to ensure the safety of research participants and the integrity of the study data.. The study staff (PI, Co-Investigators, research nursing, etc.) are responsible for collecting and recording all clinical data. As these results are collected, all toxicities and adverse events will be identified, graded for severity and assigned causality, reported to the required entities, and compiled for periodic review. After assigning causality, the PI will decide the course of action for the study participant. The PI will evaluate all adverse events (AE) and determine whether the AE affects the risk/benefit ratio of the study and whether modifications to the protocol or informed consent form are required.

10.2 Image Quality Evaluation: Images will be computed in Radiation Oncology within 2-3 days of 4DCT acquisition. The investigators will perform QA of the images directly after computation. If the imaging is not evaluable, the investigator will inform the research staff and an additional patient will be acquired.

10.3 Toxicity Grading. The Common Terminology Criteria for Adverse Events version 4.0 will be used to grade all (CTCAE v4.0; available at http://ctep.cancer.gov/protocolDevelopment/electronic_applications/ctc.htm) treatment-related adverse events. All patient encounter or treatment areas should have access to a copy of these criteria.

10.4 Adverse Events. All AE's (or unanticipated events) must be reported to the Protocol PI. All serious adverse events, defined as grade 4 or 5 toxicity, will be reported to the Beaumont Health System's IRB (institutional review board) of according to institutional reporting guidelines and using institutional reporting forms. Reports of serious adverse events will be delivered to Clinical Research Compliance and will be submitted to the U.S. Food and Drug Administration by the safety coordinator according to 21CFR 312.32.

10.5 AE Reporting. The following AEs experienced by patients accrued to this protocol and attributable to the protocol treatment (definitely, probably, or possibly related) should be reported.

10.5.1 Death on study.
10.5.2 Hospitalization or prolongation of hospitalization on study
10.5.3 Life-threatening event
10.5.4 Persistent or significant disability or incapacity

11.0 DATA CONFIDENTIALITY PLAN

11.1 All patient-reported outcome, laboratory, radiographic, and clinical data gathered in this protocol will be stored in a password-protected database. All patient information will be handled using anonymous identifiers. Linkage to patient identity is only possible after accessing a password-protected database. Access to the database is only available to individuals directly involved in the study. Information gathered for this study will not be reused or disclosed to any other person or entity, or for other research. Once the research has been completed, identifiers will be retained for as long as is required by law and by institutional regulations, and at that point will be destroyed.

12.0 REFERENCES:

1. Goldhaber SZ, Bounameaux H. Pulmonary embolism and deep vein thrombosis. The Lancet.379(9828):1835-46. doi: 10.1016/S0140-6736(11)61904-1.
2. Dismuke SE, Wagner EH. Pulmonary embolism as a cause of death. The changing mortality in hospitalized patients. Jama. 1986;255(15):2039-42. Epub 1986/04/18. PubMed PMID: 3959287.
3. Zhan C, Miller MR. Excess length of stay, charges, and mortality attributable to medical injuries during hospitalization. Jama. 2003;290(14):1868-74. Epub 2003/10/09. doi: 10.1001/jama.290.14.1868. PubMed PMID: 14532315.
4. Venous thromboembolism in adult hospitalizations - United States, 2007-2009. MMWR Morbidity and mortality weekly report. 2012;61(22):401-4. Epub 2012/06/08. PubMed PMID: 22672974.
5. Grosse SD, Nelson RE, Nyarko KA, Richardson LC, Raskob GE. The economic burden of incident venous thromboembolism in the United States: A review of estimated attributable healthcare costs. Thrombosis research. 2016;137:3-10. Epub 2015/12/15. doi: 10.1016/j.thromres.2015.11.033. PubMed PMID: 26654719; PMCID: Pmc4706477.
6. Anderson DR, Kahn SR, Rodger MA, Kovacs MJ, Morris T, Hirsch A, Lang E, Stiell I, Kovacs G, Dreyer J, Dennie C, Cartier Y, Barnes D, Burton E, Pleasance S, Skedgel C, Oâ€™Rouke K, Wells PS. Computed Tomographic Pulmonary Angiography vs Ventilation-Perfusion Lung Scanning in Patients With Suspected Pulmonary Embolism. JAMA. 2007;298(23):2743-53. doi: 10.1001/jama.298.23.2743.
7. Anderson DR, Barnes DC. Computerized tomographic pulmonary angiography versus ventilation perfusion lung scanning for the diagnosis of pulmonary embolism. Current opinion in pulmonary medicine. 2009;15(5):425-9.
8. Stein PD, Fowler SE, Goodman LR, Gottschalk A, Hales CA, Hull RD, Leeper KV, Jr., Popovich J, Jr., Quinn DA, Sos TA, Sostman HD, Tapson VF, Wakefield TW, Weg JG, Woodard PK, the PIII. Multidetector Computed Tomography for Acute Pulmonary Embolism. N Engl J Med. 2006;354(22):2317-27. doi: 10.1056/NEJMoa052367.
9. Stein PD, Woodard PK, Weg JG, Wakefield TW, Tapson VF, Sostman HD, Sos TA, Quinn DA, Leeper KV, Jr., Hull RD, Hales CA, Gottschalk A, Goodman LR, Fowler SE, Buckley JD. Diagnostic Pathways in Acute Pulmonary Embolism: Recommendations of the PIOPED II Investigators. Radiology. 2007;242(1):15-21. doi: 10.1148/radiol.2421060971.
10. Le Roux P-Y, Robin P, Delluc A, Abgral R, Le Duc-Pennec A, Nowak E, Couturaud F, Le Gal G, Salaun P-Y. V/Q SPECT Interpretation for Pulmonary Embolism Diagnosis: Which Criteria to Use? Journal of Nuclear Medicine. 2013;54(7):1077-81.
11. Phillips JJ, Straiton J, Staff RT. Planar and SPECT ventilation/perfusion imaging and computed tomography for the diagnosis of pulmonary embolism: A systematic review and meta-analysis of the literature, and cost and dose comparison. European Journal of Radiology. 2015;84(7):1392-400. doi: http://dx.doi.org/10.1016/j.ejrad.2015.03.013.
12. Wagner HN, Jr., Sabiston DC, Jr., McAfee JG, Tow D, Stern HS. Diagnosis of massive pulmonary embolism in man by radioisotope scanning. N Engl J Med. 1964;271:377-84. PubMed PMID: 14164654.
13. Petersson J, Sanchez-Crespo A, Larsson SA, Mure M. Physiological imaging of the lung: single-photon-emission computed tomography (SPECT). J Appl Physiol. 2007;102(1):468-76. doi: 10.1152/japplphysiol.00732.2006.
14. Harris RS, Schuster DP. Visualizing lung function with positron emission tomography. J Appl Physiol. 2007;102(1):448-58. doi: 10.1152/japplphysiol.00763.2006.
15. Fink C, Ley S, Risse F, Eichinger M, Zaporozhan J, Buhmann R, Puderbach M, Plathow C, Kauczor H-U. Effect of Inspiratory and Expiratory Breathhold on Pulmonary Perfusion:

Assessment by Pulmonary Perfusion Magnetic Resonance Imaging. . Invest Radiol. 2005;40(2):72-9.
16. Damen EMF, Muller SH, Boersma LJ, de Boer RW, Lebesque JV. Quantifying Local Lung Perfusion and Ventilation Using Correlated SPECT and CT Data. J Nucl Med. 1994;35(5):784-92.
17. Scarfone C, Jaszczak RJ, Gilland DR, Greer KL, Munley MT, Marks LB, Coleman RE. Quantitative pulmonary single photon emission computed tomography for radiotherapy applications. Medical Physics. 1999;26(8):1579-88.
18. O'Connor MK, Kemp BJ. Single-Photon Emission Computed Tomography/Computed Tomography: Basic Instrumentation and Innovations. Semin Nucl Med. 2006;36(4):258-66.
19. Lu Y, Lorenzoni A, Fox JJ, Rademaker J, Vander Els N, Grewal RK, Strauss HW, Schoder H. Noncontrast perfusion single-photon emission CT/CT scanning: a new test for the expedited, high-accuracy diagnosis of acute pulmonary embolism. Chest. 2014;145(5):1079-88. Epub 2014/05/07. doi: 10.1378/chest.13-2090. PubMed PMID: 24798835.
20. Yoshida S, Wu D, Fukumoto M, Akagi N, Seguchi H. Quantitative study of the difference in pulmonary perfusion in different respiratory phases in healthy volunteers. Ann Nucl Med. 2002;16(8):533-9. PubMed PMID: 12593418.
21. Suga K, Kawakami Y, Iwanaga H, Hayashi N, Seto A, Matsunaga N. Comprehensive Assessment of Lung CT Attenuation Alteration at Perfusion Defects of Acute Pulmonary Thromboembolism With Breath-Hold SPECT-CT Fusion Images. J Comput Assist Tomogr. 2006;30(1):83-91.
22. Liang J, Jarvi T, Kiuro A, Kormano M, Svedstrom E. Dynamic chest image analysis: Model-based perfusion analysis in Dynamic Pulmonary Imaging. EURASIP JASP. 2003;2003(5):437-48.
23. Simon BA. Non-invasive imaging of regional lung function using x-ray computed tomography. J Clin Monit Comput. 2000;16(5-6):433-42. PubMed PMID: 12580227.
24. Castillo R, Castillo E, Martinez J, Guerrero T. Ventilation from four dimensional computed tomography: density versus jacobian methods. Phys Med Biol. 2010;55(16):4661 - 85.
25. Guerrero TM, Sanders K, Martinez J, Castillo E, Zhang Y, Tapia R, Guerra R, Borghero Y, Komaki R. Quantification of regional ventilation from treatment planning CT. Int J Radiat Oncol Biol Phys. 2005;62(3):630 - 4.
26. Guerrero TM, Sanders K, Castillo E, Zhang Y, Bidaut L, Pan T, Komaki R. Dynamic ventilation imaging from four-dimensional computed tomography. Phys Med Biol. 2006;51(4):777-91. PubMed PMID: 16467578.
27. Brecher GA, Hubay CA. Pulmonary blood flow and venous return during spontaneous respiration. Circ Res. 1955;3(2):210-4. Epub 1955/03/01. PubMed PMID: 14352406.
28. Pinsky MR. Heart lung interactions during mechanical ventilation. Current opinion in critical care. 2012;18(3):256-60. Epub 2012/04/05. doi: 10.1097/MCC.0b013e3283532b73. PubMed PMID: 22473256.
29. Cao JJ, Wang Y, Schapiro W, McLaughlin J, Cheng J, Passick M, Ngai N, Marcus P, Reichek N. Effects of respiratory cycle and body position on quantitative pulmonary perfusion by MRI. J Magn Reson Imaging. 2011;34(1):225-30. Epub 2011/06/24. doi: 10.1002/jmri.22527. PubMed PMID: 21698712.
30. Reinhardt JM, Ding K, Cao K, Christensen GE, Hoffman EA, Bodas SV. Registration-based estimates of local lung tissue expansion compared to xenon CT measures of specific ventilation. Med Img Anal. 2008;12(6):752-63.
31. Cournand A. Pulmonary circulation; its control in man, with some remarks on methodology. Science (New York, NY). 1957;125(3260):1231-5. PubMed PMID: 13432788.
32. Fink C, Ley S, Risse F, Eichinger M, Zaporozhan J, Buhmann R, Puderbach M, Plathow C, Kauczor HU. Effect of inspiratory and expiratory breathhold on pulmonary perfusion:

assessment by pulmonary perfusion magnetic resonance imaging. Invest Radiol. 2005;40(2):72-9. PubMed PMID: 15654250.
33. Pinsky MR. Determinants of pulmonary arterial flow variation during respiration. Journal of Applied Physiology. 1984;56(5):1237.
34. Seely RD. Dynamic effect of inspiration on the simultaneous stroke volumes of the right and left ventricles. The American journal of physiology. 1948;154(2):273-80. Epub 1948/08/01. PubMed PMID: 18893088.
35. Keall PJ, Starkschall G, Shukla H, Forster KM, Ortiz V, Stevens C, Vedam SS, George R, Guerrero TM, Mohan R. Acquiring 4D thoracic CT scans using a multislice helical method. Physics in Medicine and Biology. 2004;49(10):2053-67.
36. Pan T. Comparison of helical and cine acquisitions for 4D-CT imaging with multislice CT. Med Phys. 2005;32(2):627-34. PubMed PMID: 15789609.
37. Dice R. Measure of the amount of ecological association between species. Ecology. 1945;26(2):297-302.
38. Zou KH, Warfield SK, Bharatha A, Tempany CMC, Kaus MR, Haker SJ, Wells WM, Jolesz FA, Kikinis R. Statistical Validation of Image Segmentation Quality Based on a Spatial Overlap Index: Scientific Reports. Academic radiology. 2004;11(2):178-89. doi: 10.1016/S1076-6332(03)00671-8. PubMed PMID: PMC1415224.
39. Castillo R, Castillo E, McCurdy M, Gomez DR, Block AM, Bergsma D, Joy S, Guerrero T. Spatial correspondence of 4D CT ventilation and SPECT pulmonary perfusion defects in patients with malignant airway stenosis. Physics in Medicine and Biology. 2012;57(7):1855.
40. Obuchowski NA. ROC Analysis. American Journal of Roentgenology. 2005;184(2):364-72. doi: 10.2214/ajr.184.2.01840364.